Romanian Journal of Petroleum & Gas Technology
Vol. VII (LXXVIII) • No. 1/2026

PETROGRAPHIC AND STRUCTURAL CHARACTERIZATION OF ROCKS OUTCROPPING IN THE MAVUMA BLOCK IN ONSHORE OF THE COASTAL BASIN OF THE DEMOCRATIC REPUBLIC OF CONGO

Emmanuel Balu Phoba [1,2], François Tondozi Keto [1,2], Dona Kampata Mbwelele [1], Mathieu Matondo Mbungu [3], Phily Kazunza Mufuankol [3]

[1] Department of Exploration and Production, Faculty of Petroleum, Gas, and Renewable Energy, University of Kinshasa, Democratic Republic of Congo
[2] Geophysical Research Center (C.R.G), Department of Internal Geophysics, Kinshasa, Democratic Republic of Congo
[3] Department of Geosciences, Faculty of Science and Technology, University of Kinshasa, Democratic Republic of Congo
* Email (corresponding author): emmanuelbalu0@gmail.com

DOI: 10.51865/JPGT.2026.01.05

ABSTRACT

This research provides a petrographic and structural characterization of surface rocks in the Mavuma block, located in the terrestrial zone of the coastal basin of the Democratic Republic of Congo (DRC). The region analysed exhibits lithological diversity, incorporating both metamorphic and sedimentary rock units.

Petrographic examination of nine thin sections revealed various lithological facies, including gneisses, mica schists, amphibolites, quartzites, quartz arenites, mica metaquartzites, siltstones, grainstones, calcite-cemented sandstones, and eyed gneisses. Microscopic analysis revealed mineralogical and textural properties that suggest different rock formation mechanisms. Structural research, in conjunction with thin section examination, reveals that most crystallophyllian rocks are affected by widespread deformation characterised by extensively developed schistosity. However, some gneissic units show evidence of various deformation phases, indicating a more complicated metamorphic history.

The reconstructed structure reveals a preferred NNE-SSW direction of tectonic planes. Examination of the stress regime and fault displacement data reveals that the analysed region was mainly influenced by extensional tectonics, manifested by normal faults and associated vulnerable structures. There are also indications of previous compressive deformation, as shown by foliation features.

Keywords: petrography, structural, Mavuma block, sedimentary rocks, metamorphic rocks, coastal basin.

INTRODUCTION

The current architecture of the Earth results from numerous geological processes initiated during the Hadean eon (4600–4000 Ma), characterized by planetary differentiation, crust formation, and early evolution of the Earth's envelopes [12],[20]. Petrography plays a fundamental role in understanding these processes by providing detailed analysis of mineral

Romanian Journal of Petroleum & Gas Technology
Vol. VII (LXXVIII) • No. 1/2026

composition and rock structures, offering an integrated view of sedimentary, diagenetic, and tectonic processes that shaped sedimentary basins. In the context of the Democratic Republic of Congo's efforts to develop its natural resources, petrographic analysis contributes to the assessment of oil and mining potential while enhancing scientific knowledge of local geological structures. Mineral identification using a polarizing microscope was based on established criteria. [13],[21],[39]

The coastal basin of the Democratic Republic of Congo (DRC) represents one of the most promising sedimentary basins in terms of energy and mineral resources. Situated along the western margin of the country, it includes various geological formations, some of which are exposed at the surface in the Mavuma block. The Mavuma Block lies in the eastern part of the DRC Coastal Basin, within the Vermelha and Mavuma geological formations of Albian–Aptian age. Reconnaissance studies conducted in the eastern sector of the basin have led to mapping between longitudes 12° 35′ E and latitudes 5° 40′ S (Figure 1). Mavuma, which was the centre of deposit exploitation by the Congo Bitumen and Asphalt Company (SOBIACO) between 1950 and 1959, is located in the former Bas-Fleuve district, Lukula Territory, 65 km northeast of Muanda. [6],[7],[23],[24]

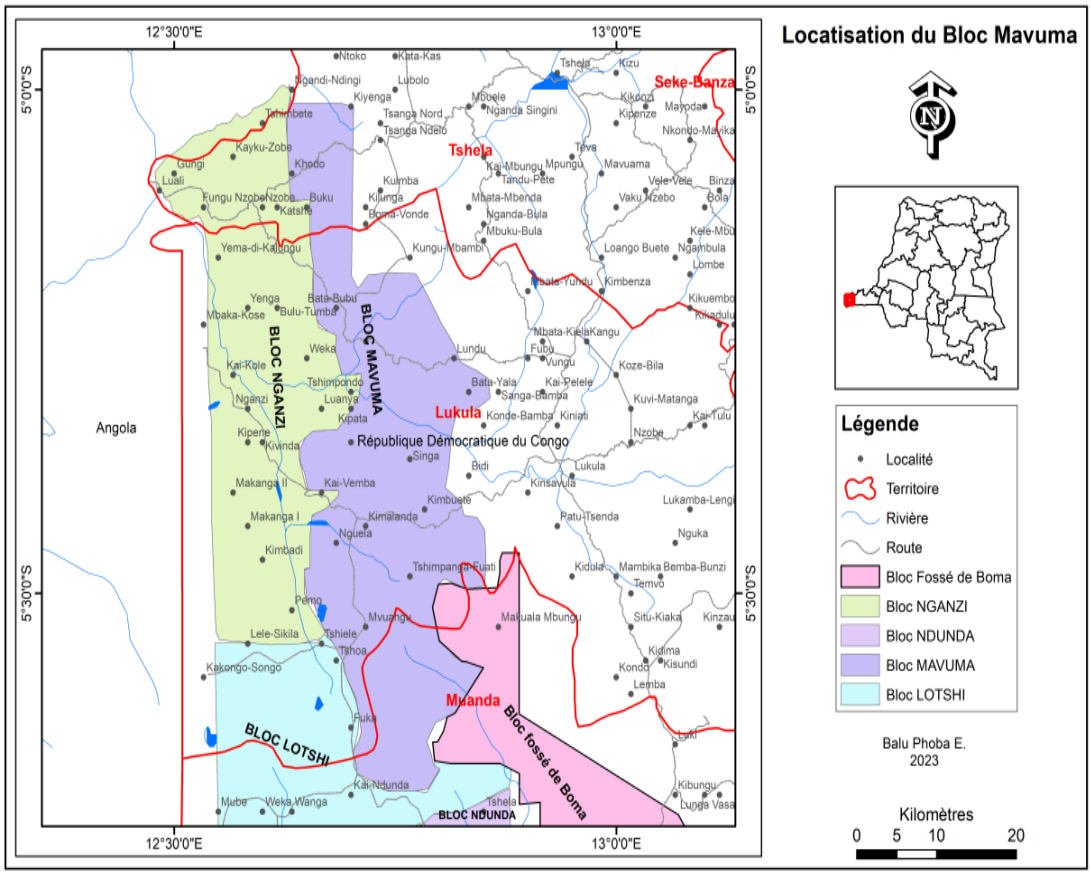

***Figure 1**. Location map of the Mavuma block*

These deposits, initially discovered in 1913, were the subject of detailed research and evaluation by the International Forestry and Mining Company of the Congo (FORMINIERE) in the 1950s [38]. Between 1980 and 1982, the Petroleum Research Works Company (SOREPZA)

reportedly conducted research into the basin's bituminous potential, with estimates indicating probable volumes of several billion cubic metres, despite the inaccessibility of accurate records. In the mid-20th century, SOBIACO conducted several geological studies in the coastal basin following its exploration projects. The existence of hydrocarbon deposits along the West African margin, from Angola to Cameroon, is closely linked to the global phenomenon of continental drift, specifically at the boundary between the African and South American plates [24].

Although the DRC's coastal basin is recognised for its hydrocarbon potential, some onshore areas, including the Mavuma block, remain poorly documented in geological terms. Existing studies have focused mainly on offshore areas or regional analyses, resulting in limited detailed information on the nature of outcropping rocks and their structural organisation. This lack of field data restricts a comprehensive understanding of the basin's tectonic and sedimentary evolution and limits the assessment of its onshore petroleum potential.

This research aims to highlight the petrographic and structural abundance of the Mavuma block formations, specifically in the Kakongo area of the Democratic Republic of Congo, by analysing rock samples taken in situ. [33] The study addresses two key questions:

- How can petrographic and structural analyses of rocks from the Mavuma block contribute to understanding the geological potential of the DRC coastal basin?
- What is the petrographic variability among the different outcrops in the block?

The working hypotheses are that the outcropping rocks of the Mavuma block exhibit lithological diversity (sedimentary, metamorphic, or igneous) reflecting the geological history of the basin, and that the structures observed (faults, folds, fractures) are the result of regional tectonic stresses linked to the basin's geodynamic evolution, influencing the distribution and orientation of rocks. [28],[30],[36],[37]

This study seeks to fill the gap by providing a detailed petrographic and structural characterisation of the outcropping rocks in the Mavuma block through direct field observations and microscopic analyses, enabling better identification of lithologies, textures, and tectonic structures. The novelty of this work lies in its integrated approach focusing on an area that has been poorly studied to date [34]. By correlating petrographic observations with geological structures, this study contributes to a more comprehensive understanding of the role of the Mavuma block in the architecture of the coastal basin and its potential importance in hydrocarbon circulation and trapping processes (Figure 2). Consequently, it constitutes an original and useful contribution to existing geological models and future onshore oil exploration activities in the DRC [7]

The geology of the coastal basin of the Democratic Republic of Congo fits within the broader context of basins on the passive margin of the west coast of Africa. The basin's structure evolved in line with rifting phenomena that occurred between the Late Jurassic and Early Cretaceous periods, marked by a complex sequence of fragmented blocks and sedimentary deposits [11],[29]. The Ante-Saliferous interval is characterised by fractured block tectonics resulting from the distension associated with the opening of the South Atlantic.

- The presence of the Saliferous corresponds to the detachment surface of the overlying cover. [8],[22]
- The post-saliferous structure is directly associated with halokinesis, which causes disharmonious swelling due to the uplift and extrusion of salt domes. [18],[32]

Romanian Journal of Petroleum & Gas Technology
Vol. VII (LXXVIII) • No. 1/2026

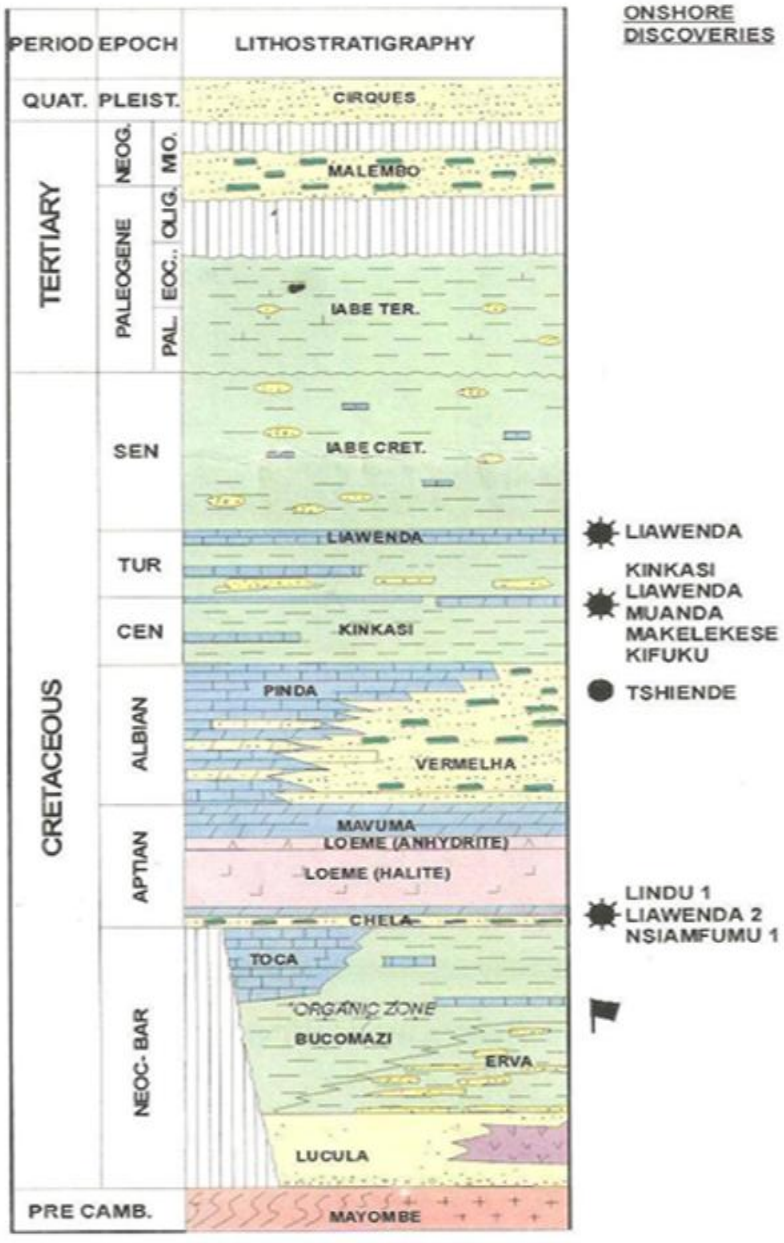

***Figure 2**. Stratigraphic log of the coastal basin of Congo* [24]

METHODS AND MATERIALS

Methods

A review of the relevant literature was conducted to establish the theoretical and geological context of the study, with particular emphasis on previous work dealing with the geology and geography of the coastal basin and the Mavuma block. The research was structured in several successive stages. The data acquisition phase consisted of a field campaign conducted in the Mavuma block, during which representative rock samples were collected from selected outcrops for subsequent analysis (Figure 3). [10],[19],[24]

Romanian Journal of Petroleum & Gas Technology
Vol. VII (LXXVIII) • No. 1/2026

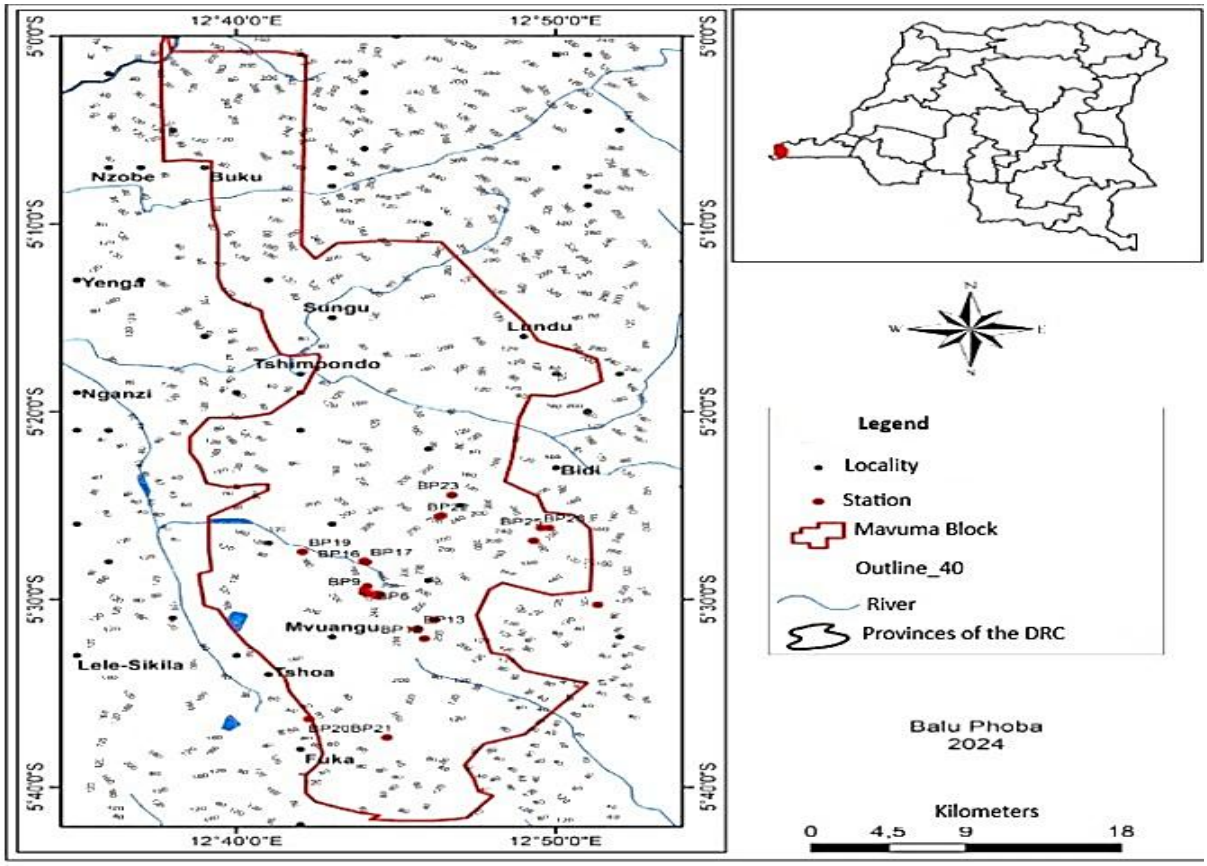

***Figure 3**. Sampling map (The red dots represent the sampling stations: BP01, BP02, BP14, BP16, BP17, BP19, BP24, BP25 and BP26)*

Following the field investigations, the collected samples were processed in the laboratories of the Faculty of Sciences, Department of Geosciences, at the University of Kinshasa. Petrographic analyses were performed using a transmitted light microscope under plane and crossed polarized light conditions. These analyses identified the mineralogical composition, textures, and microstructural relationships, enabling accurate lithological classification based on thin section observations.

The final step consisted of data processing and interpretation, focusing on the description, examination, and classification of rocks to determine their composition, structural characteristics, and geological significance. [2],[5]

Materials

The geological study of the area was conducted using specialized tools and software to accurately collect, process, and analyze the data. The geographic coordinates of the stations were recorded with a Garmin GPS, ensuring reliable georeferencing on the map. The structural and lithological information gathered in the field was integrated into ArcGIS 10.8, where it was organized and mapped to produce detailed geological maps and analyze the distribution of rock units. Furthermore, WinTensor was used to quantitatively process the structural measurements, calculating stress tensors and identifying the main deformation axes in the study area [1],[12],[19],[35]. A graphical summary of the study is shown in Figure 4.

Romanian Journal of Petroleum & Gas Technology
Vol. VII (LXXVIII) • No. 1/2026

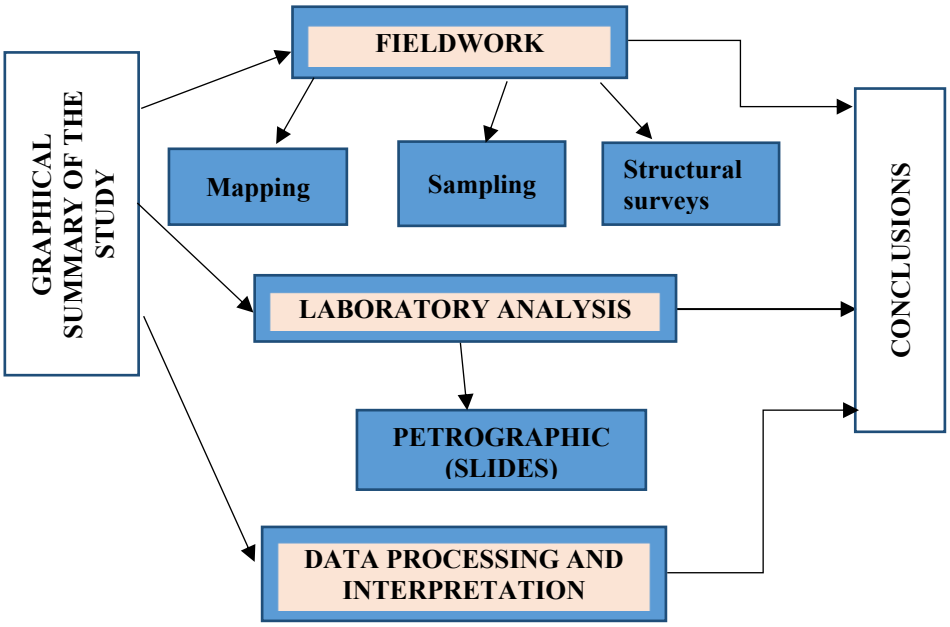

***Figure 4**. Graphical summary of the study*

RESULTS AND DISCUSSIONS

RESULTS

Description of sample BP01

Macroscopically, the rock exhibits a dark gray coloration marked by scattered whitish spots and displays a fine to medium-grained texture. Mineralogically, it is dominated by large quartz crystals disseminated within a matrix composed of dark phyllosilicate aggregates.

Microscopic examination further reveals that the rock is characterized by a well-developed foliated texture, reflecting the preferred orientation of the constituent minerals (Figure 5). This is a confused foliation supported by brown (APL – *Analyzed Polarized Light*) and dark brown (NAPL – *Non-Analyzed Polarized Light*) biotite streaks grouped in shapeless clusters and xenomorphic to subautomorphic crystals of white or gray (APL) and colorless (NAPL) quartz.

The alignment of the biotites one behind the other gives the rock two intersecting lineations, the intersection of which forms an obtuse angle. Locally, the rock also contains subcircular clusters of opaque minerals and, in places, a few rare porphyroblasts of plagioclase with polysynthetic twins (APL) and colorless (NAPL) and green hornblende (APL and NAPL). The rock is an amphibolite.

Romanian Journal of Petroleum & Gas Technology
Vol. VII (LXXVIII) • No. 1/2026

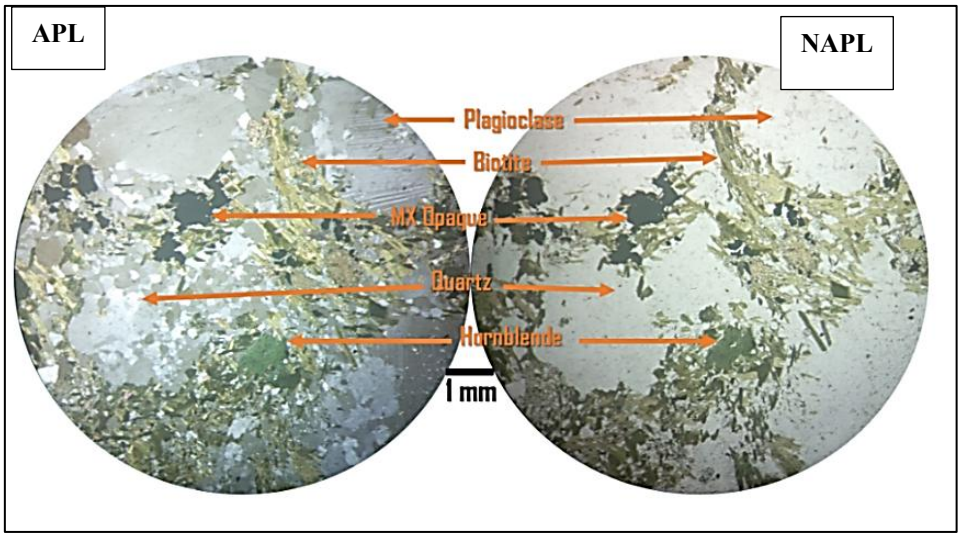

***Figure 5**. Microscopic observation of amphibolite from sample BP 01 under Analyzed Polarized Light (APL) Pl, Bt, Opq, Qz, Hbl and Non-Analyzed Polarized Light (NAPL)*

Description of sample BP 02

Macroscopically, the rock has a greyish tint and contains some traces of bitumen, while its grain size is fine and its structure massive, punctuated by coarser layers. When it comes into contact with hydrochloric acid, a slight effervescence is observed, indicating the presence of carbonate minerals in small proportions. Under the microscope (Figure 6), the rock shows a rough bedding pattern highlighted by dark brown silty-clay beds (APL and NAPL) between which subautomorphic to xenomorphic grains of white or gray quartz (APL) and colorless quartz (NAPL) are scattered. These fine sand-sized quartz grains have smooth to indented edges. The silty clay beds consist of a clay matrix impregnated with a few rare subcircular crystals of opaque minerals. The boundary between these two types of beds is sometimes interlaced and sometimes undulating. The rock is a siltstone.

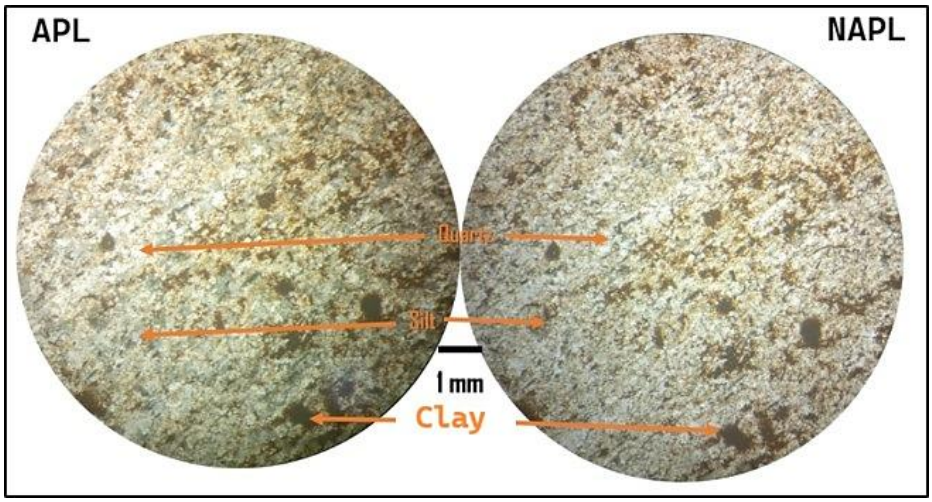

***Figure 6**. Microscopic observation of siltstone from sample B02 under Analyzed Polarized Light (APL) Qz, Ci, Cl and Non-Analyzed Polarized Light (NAPL)*

Romanian Journal of Petroleum & Gas Technology
Vol. VII (LXXVIII) • No. 1/2026

Description of sample BP14

Macroscopically, the rock has a pinkish-white color and is characterized by a succession of centimeter-thick beds, within which the fine to medium grains are dispersed relatively homogeneously. Its mineralogy is dominated by quartz and potassium feldspar, while the ferromagnesian minerals appear to follow a truncated orientation, suggesting a subtle structural organization that reflects the depositional conditions and diagenetic processes that affected the rock.

Under the microscope (Figure 7), the rock exhibits schistosity, which can be seen in the alternation of large granoblastic levels with fine lepidoblastic levels. The granoblastic levels consist of xenomorphic to subautomorphic quartz crystals that are white or gray (APL) and colorless (NAPL). The lepidoblastic layers consist of fine flakes of brown (APL) and dark brown (NAPL) biotite. The alignment of the sericite flakes one behind the other gives the rock its schistosity. The rock is a micaceous metaquartzite.

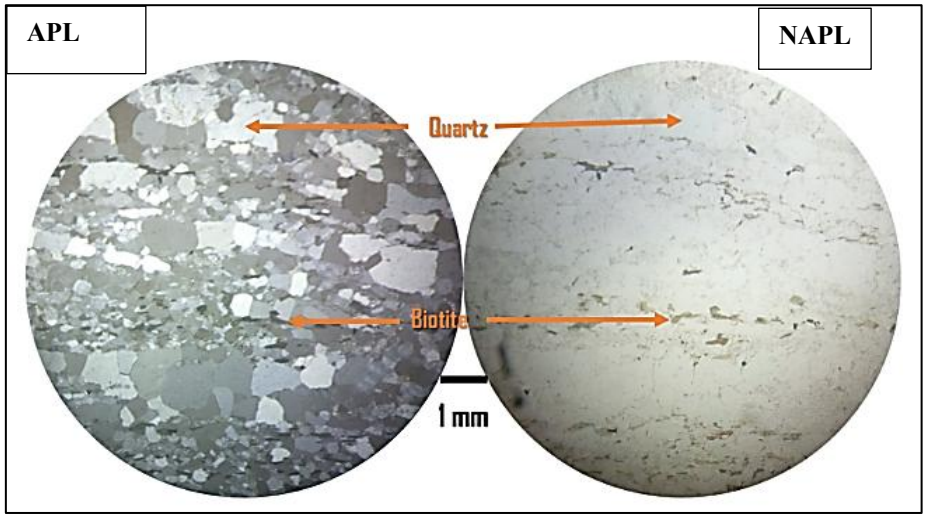

***Figure** 7. Microscopic observation of a micaceous metaquartzite from sample B14 under Analyzed Polarized Light (APL) Qz, Bt and Non-Analyzed Polarized Light (NAPL)*

Description of sample BP17

Macroscopically, the rock is distinguished by its dark color, punctuated by light-colored minerals and crystals with silvery reflections, creating an interesting visual contrast within its texture. The foliation also becomes more pronounced in certain areas, revealing a progressive organization of the minerals that appears to have resulted from both tectonic stresses and metamorphic processes that have affected the rock over time.

Under the microscope (Figure 8), the rock has a granulepideoblastic texture, evidenced by the intercalation of brown (APL) and yellow (NAPL) biotite flakes between white or gray (APL) and colorless (NAPL) quartz crystals. These fine to medium quartz crystals are generally xenomorphic. The alignment of the biotite flakes one behind the other gives the rock two schistosity planes, the intersection of which forms an obtuse angle. The rock also contains a few rare disseminated opaque mineral crystals. It is a gneiss.

Romanian Journal of Petroleum & Gas Technology
Vol. VII (LXXVIII) • No. 1/2026

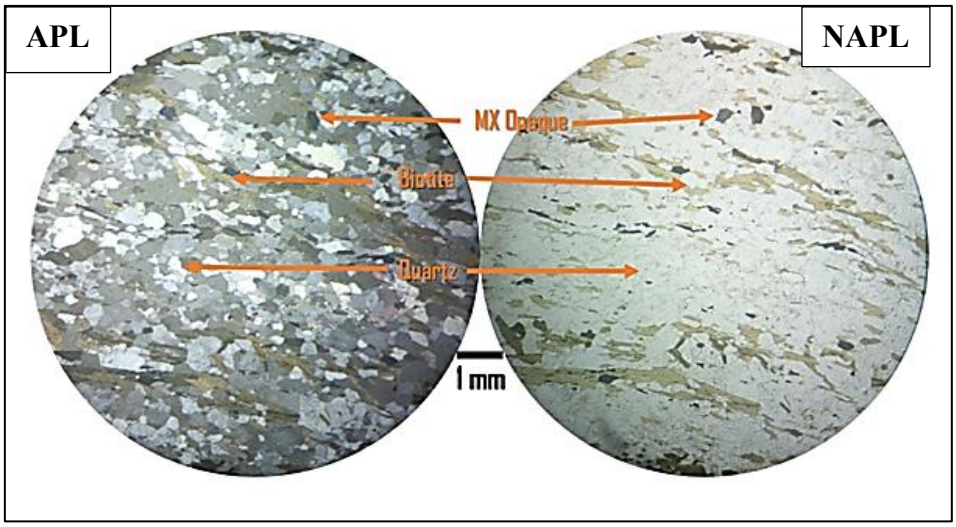

***Figure 8**. Microscopic observation of gneiss from sample BP17 under Analyzed Polarized Light (APL)Opq, Bt, Qz and Non-Analyzed Polarized Light (NAPL)*

Description of sample BP19

Macroscopically, the sample studied exhibits a relatively homogeneous gray hue, and its mineralogical composition is largely dominated by granular quartz, within which a few iron oxides appear here and there, dispersed in the matrix. Such a composition not only underscores the predominant role of quartz, but also reflects the subtle influence of accessory phases, which can subtly modulate the visual appearance and certain textural characteristics of the rock.

Under the microscope (Figure 9), the rock has a jointed texture highlighted by white or gray (APL) and colorless (NAPL) quartz grains. These quartz crystals are fine, medium, and coarse, slightly cracked in places, with angular, sub-rounded, and blunt shapes with smooth edges. Fine black lines of impurities mark the initial surface of the grains before diagenesis, on which a siliceous cement developed during compaction. The dispersion of coarse grains among medium and fine grains gives the rock a low classification [4]. It is a quartzite sandstone.

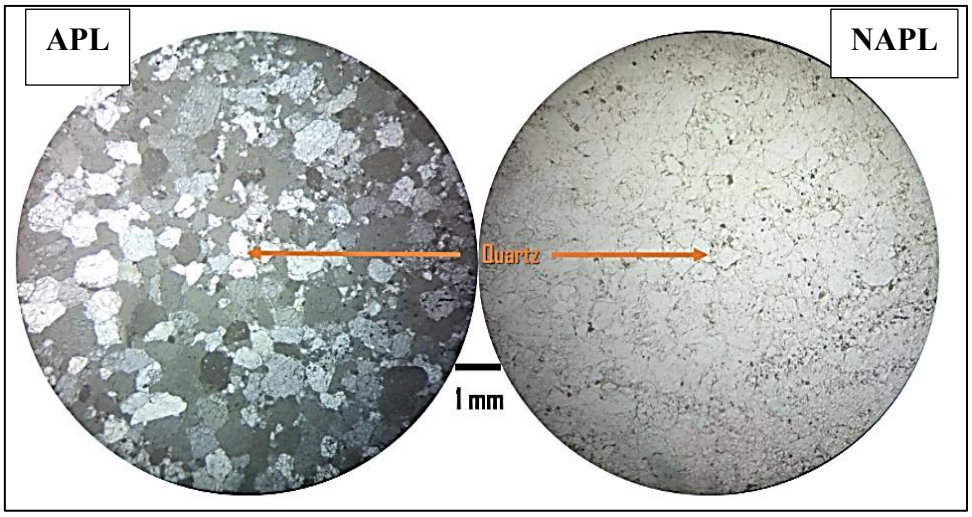

***Figure 9**. Microscopic observation of a quartzite arenite, sample BP19 under Analyzed Polarized Light (APL) Qz and Non-Analyzed Polarized Light (NAPL)*

Romanian Journal of Petroleum & Gas Technology
Vol. VII (LXXVIII) • No. 1/2026

Description of sample BP24

Macroscopically, the dark-colored rock reacts markedly to hydrochloric acid, producing effervescence, which indicates the presence of carbonate minerals. Mineralogical analysis shows that it is essentially composed of small calcite grains, whose relatively homogeneous distribution suggests a composition dominated by this carbonate phase.

Under the microscope (Figure 10), the rock exhibits a microsparitic cement containing oolites. These spherical, subspherical, and ovoid oolites are generally composed of a microsparitic nucleus covered by either a single-layer or multi-layer cortex. The single-layer cortex is sometimes composed mainly of micrite, sometimes of microsparite. The multilayered cortex consists of alternating concentric micritic and microsparitic layers. According to the classifications of Folk [17] and Dunham [14], this is a grainstone-type oomicrosparite.

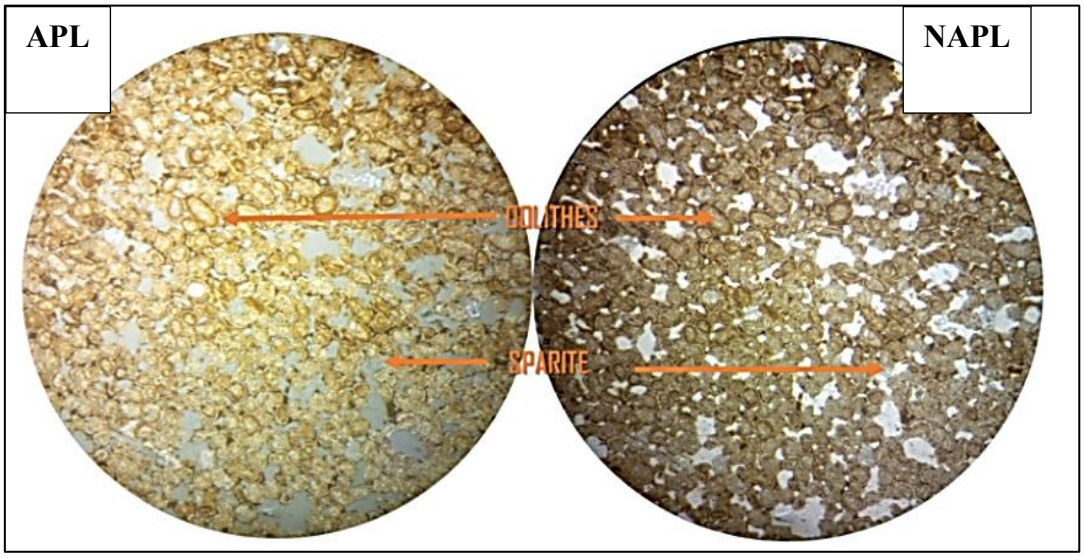

***Figure 10**. Microscopic observation of a grainstone-type oomicrosparite from sample BP24 under Analyzed Polarized Light (APL) Oo, Sp and Non-Analyzed Polarized Light (NAPL)*

Description of sample BP16

Macroscopically, in this minor channel, the rock facies gradually changes: the structure becomes increasingly foliated, and the minerals are arranged in a clearly oriented manner. This evolution is reflected in a visible alternation between dark layers, rich in ferromagnesian minerals, and lighter layers, dominated by quartz and potassium feldspar, highlighting the diversity of texture and mineralogical composition. Furthermore, the rock blocks exhibit a grain size ranging from fine to medium, reflecting the variety of processes that have contributed to shaping this internal organization.

Under the microscope (Figure 11), the rock exhibits schistosity, as evidenced by alternating layers of lepidoblastic foliation and large quartz levels. The lepidoblastic foliation consists of brown (APL) and brown to colorless (NAPL) biotite flakes. The granoblastic layers consist of small to medium-sized quartz crystals that are white or gray (APL) and colorless (NAPL). These fine to medium-sized quartz crystals are xenomorphic, automorphic, and sometimes elongated. The rock is a mica schist.

Romanian Journal of Petroleum & Gas Technology
Vol. VII (LXXVIII) • No. 1/2026

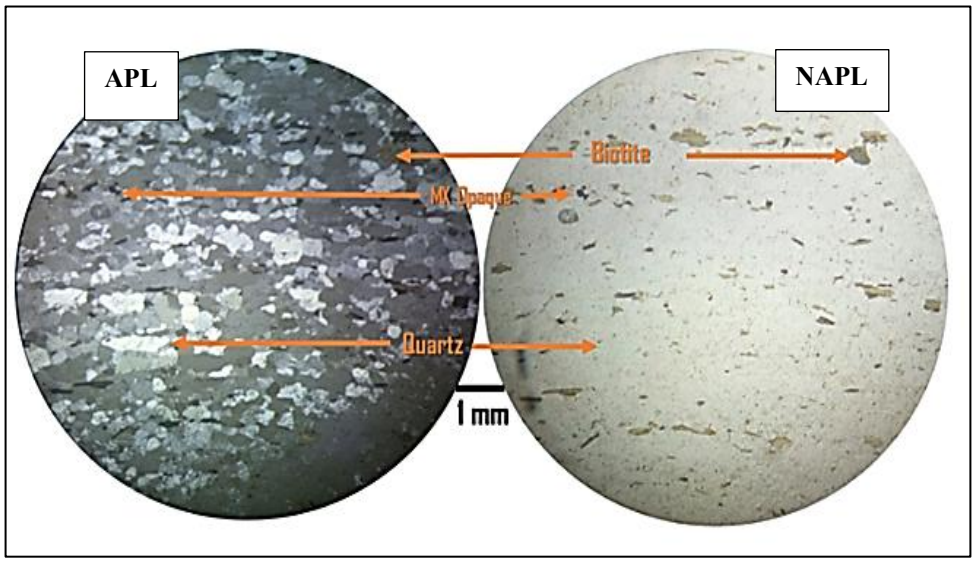

Figure 11. *Microscopic observation of a mica schist from sample BP16 under Analyzed Polarized Light (APL) Bt, Opq, Qz and Non-Analyzed Polarized Light (NAPL)*

Description of sample BP25

Macroscopically, the rock exhibits a foliated structure characterized by alternating light-colored layers, primarily composed of quartz, muscovite (or sericite), and orthoclase, and darker layers dominated by phyllite-textured ferromagnesian minerals. Large, sometimes ocular-shaped, crystals are also scattered throughout, detaching from the matrix and contributing to the variation in the sample's texture.

Under the microscope (Figure 12), the rock exhibits confused foliation. This is evident in the alignment of brown (APL) and dark brown (NAPL) biotite flakes that intersect with each other. These flakes are intercalated between white or gray (APL) and colorless (NAPL) quartz crystals. The alignment of the biotite flakes one behind the other gives the rock two linear structures. The fine to medium quartz crystals are xenomorphic to subautomorphic. Locally, the rock contains small subautomorphic crystals of opaque minerals. The rock is a gneiss.

Description of sample BP26

Macroscopically, the rock sample shows a strongly foliated structure, dominated by silky-looking phyllites, corresponding to sericite. The rock naturally breaks into platelets, highlighting the preferential orientation of the minerals within the foliated structure.

The thin section (Figure 13) shows a sandstone detrital rock consisting mainly of subangular to subrounded quartz grains, fine to medium in size, arranged in a grain-supported texture. The intergranular cement is abundant and consists mainly of calcite, recognizable under polarized light analysis by its high multicolored interference colors. Locally, there are a few secondary minerals such as chlorite (greenish hues) and a few scattered opaque grains. The primary porosity is greatly reduced by carbonate cementation. The rock is interpreted as a quartz sandstone with calcareous cement.

Romanian Journal of Petroleum & Gas Technology
Vol. VII (LXXVIII) • No. 1/2026

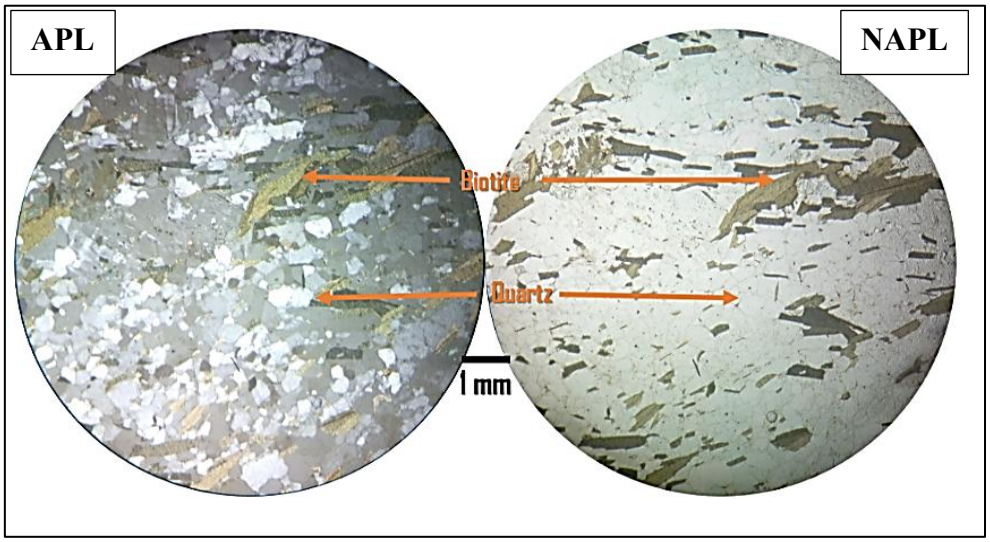

Figure 12. *Microscopic observation of gneiss from sample BP25 under Analyzed Polarized Light (APL) Bt, Qz and Non-Analyzed Polarized Light (NAPL)*

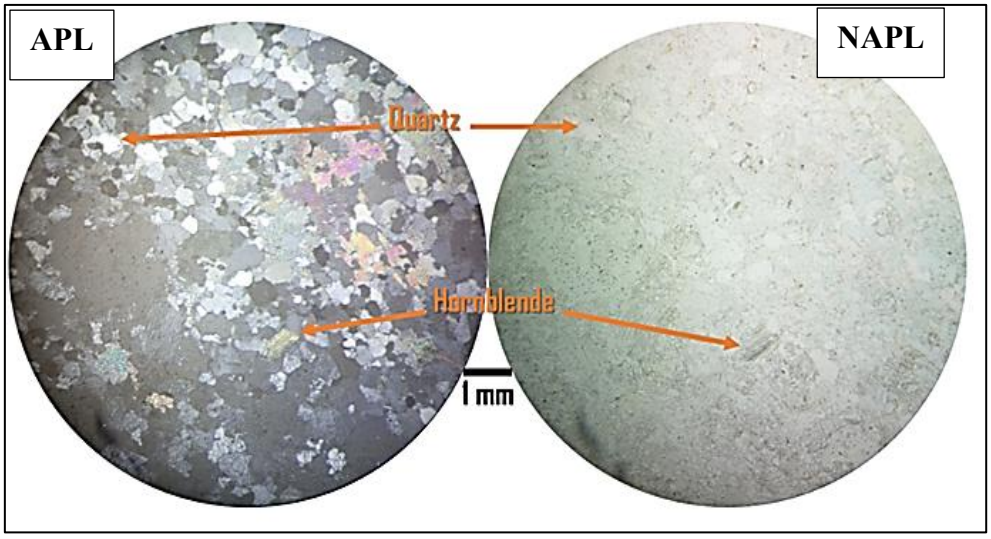

Figure 13. *Microscopic observation of quartz sandstone with calcium cement from sample BP26 under Analyzed Polarized Light (APL) Qz, Hbl and Non-Analyzed Polarized Light (NAPL)*

Presentation of Structural Data

Table 1 shows the orientations of fracture planes (FP), stratification planes (SP), foliation planes (FP1), and schistosity planes (SP1) observed in the formations outcropping in the study area.

Romanian Journal of Petroleum & Gas Technology
Vol. VII (LXXVIII) • No. 1/2026

Table 1. *Presenting structural data in the Mavuma block.*

Station Number	Fracturing plan	Stratification plane	Foliation plane	Schistosity plane
BP03	N192°/38°			
BP07	N348°/80°			
BP10		N 135°/60°		
BP11		N 154°/60°		
BP14	N 47°/90° N 342°/80°	N 190°/40°		
BP15	N 150°/90° N 144°/80°			
BP16	N144°/80° N20°/58°		N 190°/40°	
BP17				N 169°/22°
BP 19		N 296°/34°		
BP24		N 266°/4°		
BP25	N 12°/90°		N 314°/20°	
BP26				N 11°/19°

- **Results of the principal axes of the stress tensor Axis Orientation Azimuth/Dip derived from fracture planes.**

These structural data are processed using Win Tensor software, as mentioned above. Approximately nine structural elements were considered and plotted in the Wulf grid. Analysis of these different tectonic planes reveals a preferential NNE-SSW direction (Figure 14). Most of the planes have a dip between 20° and 90°, which shows an inclination of the structures (both continuous and discontinuous).

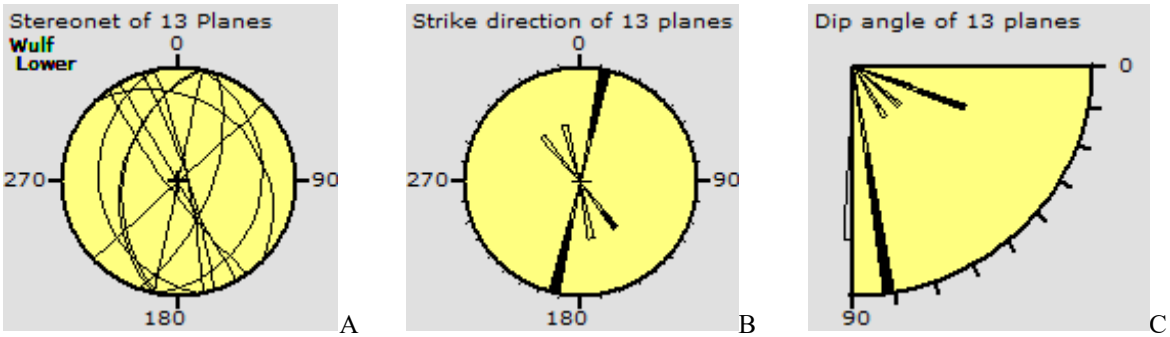

Figure 14*. Stereonet showing the synthesis of the different orientations of the structural elements (A); their different orientations (B) and their dips (C).*

The region exhibits various tectonic deformations, including: an earlier folding (orogenesis), evidenced by the presence of schistosity and foliation, A network of discontinuities (generally joints, diaclases, and normal faults) represented by two main families showing dips to the northwest and southeast, respectively. [25]

Figure 14 shows the results obtained after analysing all the structural elements to determine the stress tensor. Knowing the measurements of these structural elements, it is therefore possible to reconstruct the stress state that produced them [1]. In this case, we used the rotational optimization method with the *F*5 minimization function (R. Optm. F5).

Based on the tectonic inversion method, the three main stress axes causing the activation of the faults have the following orientations:

- σ1: N194°/67°, subvertical principal stress oriented NNE-SSW;
- σ2: N341°/20°, weakly inclined intermediate stress, oriented SSE-NNW with an average dip;
- σ3: N75°E/12°, minimal subhorizontal stress, oriented WSW-ENE with a very weak dip.

The shape ratio index R, calculated based on these three stresses using the formula R = (σ2 – σ3) / (σ1 – σ3), is used to determine the tectonic regime index (R'), which defines the type of stress regime (extensive, detachment, or compressive) in the region. Thus:

- If $0<R'<1$, the regime is distensive with a normal fault (NF);
- If $1<R'<2$, the regime is compressive with shearing (SS);
- If $2<R'<3$, the regime is compressive with a reverse fault (TF).

The maximum stress has the greatest dip and tends to be vertical, while the secondary stress has a low value. Thus, when σ1> σ2> σ3, $R' = R$ for the extensive regime (normal faults: NF).

Figure 14 shows us a shape ratio index value of $R = 0.85$, so the tectonic regime index will be: $R' = R = 0.85$ (extensive regime).

Structural data analysis was performed using Wulff's stereographic projection, which was later formalized in the field of structural geology [31]. This method made it possible to visualize and analyse the measured structural elements.

The ternary diagram (NF-SS-TF) (Figure 15) shows that our region was last affected by extensive deformation (normal faults NF, joints, and diaclases), but also that it initially evolved under compression, which would have left foliation markers. The red dots on the image show the direction of stress, while the blue dots define the direction of maximum deformation.

Examination of the detected tectonic patterns shows a predominant NNE-SSW direction, suggesting a preferential structural inclination in the area under study. The ternary diagram (NF-SS-TF), linked to the tectonic regime index *R*', indicates that the area has recently undergone extensional deformation, as evidenced by the dominant presence of normal faults (NF), joints, and fractures.

- **PBT axis (Tension axis / σ3)**

The PBT axis gives the following orientation: N264°/88° (SSE-NNW) this is very consistent with σ3, confirming the extensive regime (Figure 16). Reduced stress tensor after inversion of fracture plane data using the PBT axis method.

- **Horizontal components (SHmax / SHmin)**

SHmax = 166° → horizontal stresses therefore extend perpendicular to ENE–WSW.

SHmin: zero but implicit (orthogonal); In an extensive regime, σ1 is vertical and SHmin ≈ σ3.

Romanian Journal of Petroleum & Gas Technology
Vol. VII (LXXVIII) • No. 1/2026

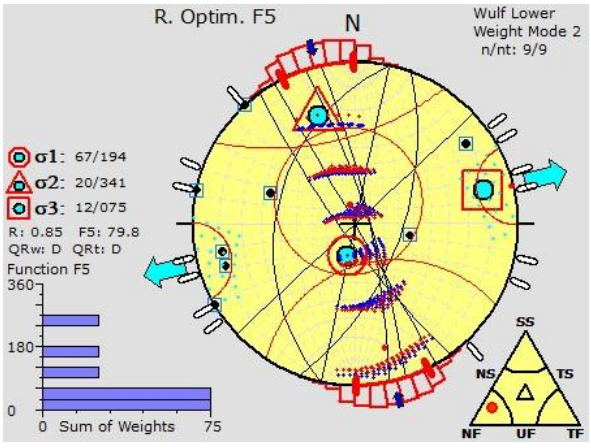

***Figure 15**. Stress tensor of the various tectonic deformations in the region.*

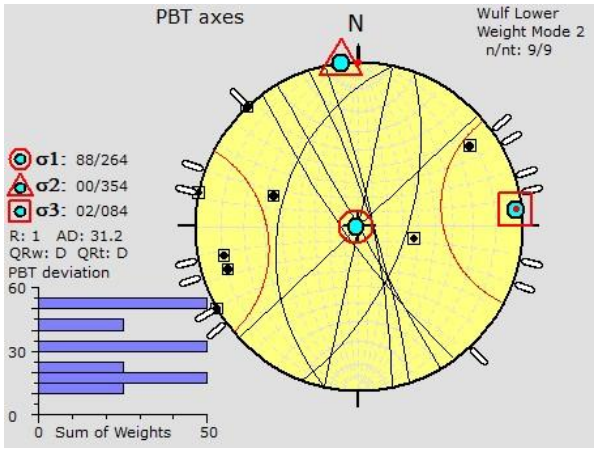

***Figure 16**. Reduced stress tensor after inversion of fracture plane data using the PBT axes method*

DISCUSSION

Sedimentary Characteristics of Carbonate Lithofacies

Petrographic analysis of the samples, particularly BP24, reveals three major characteristics: oolites, grainstone texture, and black coloration.

Oolites: The oolites exhibit a concentric and homogeneous structure. They form in shallow (0–12 m) turbulent waters, in marine environments, sometimes in lagoons or lakes [16]. Their presence indicates an environment where currents and waves are sufficient to keep grains in suspension and promote their concentric growth.

Grainstone Texture: The grainstone texture observed in BP24, composed of oolitic debris, confirms a dynamic sedimentation environment. The hydrodynamic conditions were strong enough to sort the grains and create grainstone structures typical of lower to mid-tidal zones [16].

Black coloration: The black coloration of the sample reflects reducing conditions and low oxygen content. These conditions allowed for the preservation of organic matter, corroborated by the presence of traces of bitumen [16].

The combination of these three characteristics suggests a shallow but dynamic marine environment, with intense hydrodynamics and low-oxygenation zones that favor the preservation of organic matter.

Metamorphic Characteristics

The study of thin sections did not reveal any sillimanite, kyanite, andalusite, or cordierite silicates that could serve as indicators for directly assessing the level of metamorphism to which the rocks were subjected. In the absence of these standard minerals, the parageneses observed can nevertheless be used to assess the level of metamorphism (Figure 17).

Depending on the variations in the pressure-temperature curve (Figure 18), specific metamorphic facies can be linked to the mineral parageneses of the rocks examined. These facies, which evolve according to pressure and temperature, were initially categorized for mafic rocks and form the basis for interpreting metamorphic conditions [15].

Romanian Journal of Petroleum & Gas Technology
Vol. VII (LXXVIII) • No. 1/2026

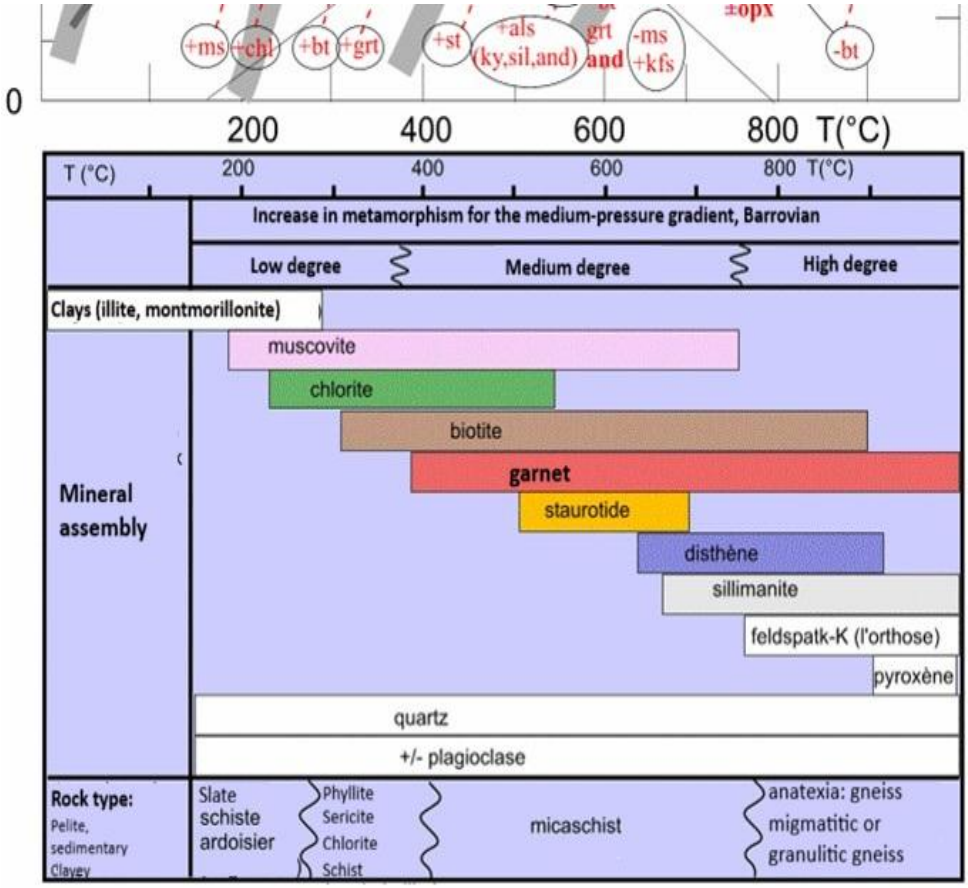

***Figure 17**. Diagram showing the evolution of minerals with the intensity of metamorphism* [26]

The following mineral parageneses have been identified in our study area:

- The sericite-quartz paragenesis is characteristic of sericite schist. It is typical of green schist facies according to the diagram by Nicholet [26]. This rock would have formed during low-grade metamorphism of a silopelitic sequence in which the clay minerals were transformed into sericite and the quartz grains underwent simple recrystallization. [34]
- The opaque minerals present in these rocks are either sulfides or chlorides deposited by metamorphic fluids [31].
- The hornblende-plagioclase association is associated with amphibolite lithofacies. Hornblende coupled with the presence of plagioclase reflects the evolution of this rock at the boundary between amphibolite facies and granulite facies (Figure 18). Its brown color (of the amphibolite blade) is diagnostic of titanium enrichment, indicating that it belongs to the medium degree of metamorphism in the amphibolite facies domain.
- The mineralogical association of quartz, biotite, and opaque minerals is characteristic of single-mica mica schist (sample BP16). Quartz is a ubiquitous mineral (Figure 17), and biotite as the characteristic index mineral of the mesozone. [3]

Romanian Journal of Petroleum & Gas Technology
Vol. VII (LXXVIII) • No. 1/2026

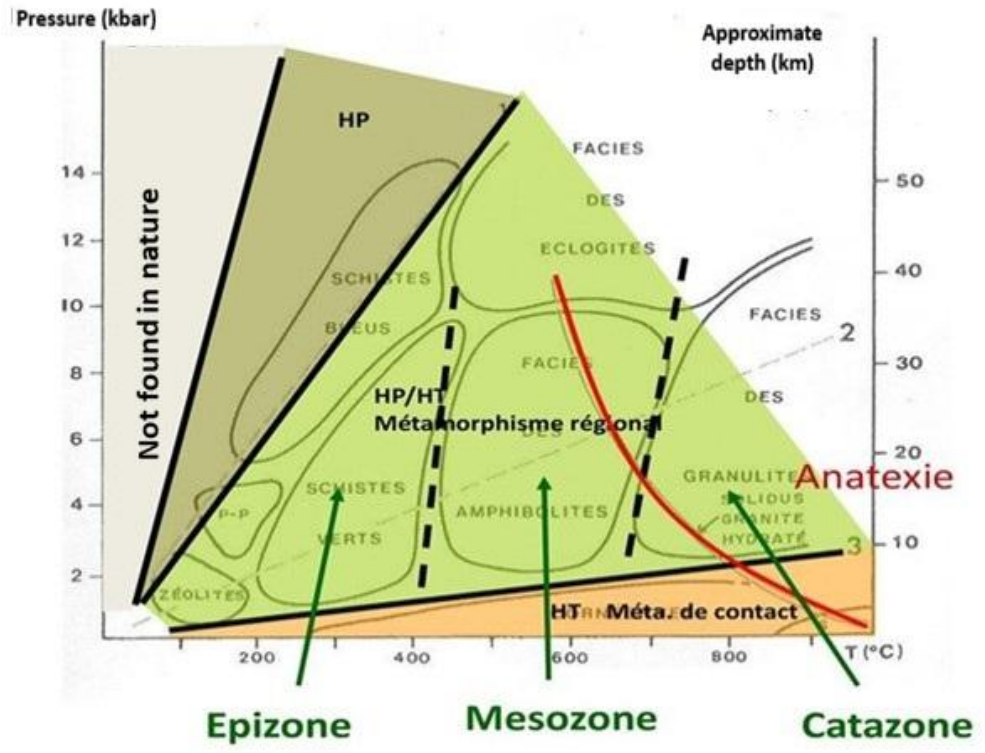

***Figure 18**. Diagram showing the different metamorphic zones.* [26]

Tectonic Consequences and Chronology of Deformation

The rocks studied (amphibolites, sericite schists, mica schists, gneisses) exhibit a unique schistosity, suggesting a single episode of regional deformation. This episode corresponds to the Pan-African orogeny that affected the West Congo Supergroup during the Neoproterozoic [9],[27],[40]. The epizonal and mesozonal rocks exhibiting a unique schistosity are attributed to the Mayumbian and Zadinian groups of the West Congo Supergroup. This interpretation directly links the petrographic and metamorphic observations to a coherent regional tectonic context.

CONCLUSIONS

This study enabled us to carry out a petrographic and structural characterization of the rocks outcropping in the Mavuma block of the coastal basin of the Democratic Republic of Congo. Macroscopic and microscopic analyses revealed lithological units belonging to metamorphic and sedimentary rock groups. These include gneiss, mica schist, amphibolite, quartzite, quartz sandstone, micaceous metaquartzite, siltstone, grainstone, and quartz sandstone cemented by calcite.

The observed schistosity can be interpreted as consistent with the regional-time deformation that affected the formations of the Pan-African Neoproterozoic Supergroup of western Congo. The metamorphic assemblages and structural features imply epizonal to mesozonal conditions in the area.

The extensive tectonic regime is characterized by a reconstructed stress field, where the maximum principal stress is subvertical (σ1) and the minimum principal stress is subhorizontal (σ3). The calculation of the stress ratio (R' = 0.85) confirms the analysis of a normal fault associated with this stage of deformation.

The directions of the principal stress axes, derived from the inversion of the stress tensor, reveal a consistent stress configuration. Furthermore, the results obtained from various analytical methods show a high degree of agreement, which reinforces the credibility of the reconstructed tectonic regime. From a geodynamic perspective, the detected extension regime is consistent with post-orogenic relaxation.

Overall, the results provide new petrographic and structural information derived from the field for a poorly documented area of the DRC coastal basin and offer constraints for future geological and tectonic analyses of the Mavuma block.

REFERENCES

[1] Angelier, J., Direct inversion and 4-D restoration: Physical and mathematical comparison of methods for determining paleostress tensors from fault data. Comptes Rendus de l'Académie des Sciences, 312(11), 1213–1218. 1991.

[2] Bertrand, J.M., Bertrand-Sarfati, J., Bessoles, B., Black, R., Fabre, J., West Africa: Geological Introduction and Stratigraphic Terminology. Pergamon Press, Oxford. 1983.

[3] Boillot, J.P. & al., Mineralogical and metamorphic characterization of mesozonal metamorphism: biotite as an indicator mineral. Document non publié / rapport technique, année 2020. Cité dans Benjamin & Luteta (2022).

[4] Bott, M.H.P., The mechanism of oblique-slip faulting. Geological Magazine, 96, 109–117. 1959.

[5] Byerlee, J.D., Friction of rocks. Pure and Applied Geophysics, 116, 615–626. 1978.

[6] Cahen, L., Lepersonne, J., État actuel des connaissances relatives aux séries mésozoïques de l'intérieur du Congo. Bulletin de la Société Belge de Géologie, 87, 20–37. 1954.

[7] Caillaud, A., Blanpied, C., Guillocheau, F., Delvaux, D., The Jurassic Stanleyville Formation on the eastern margin of the Congo Basin. Journal of African Earth Sciences, 132, 80–98. 2017.

[8] Cello, G., Mazzoli, S., Tondi, E., Turco, E., Active tectonics of the central Apennines. Tectonophysics, 272, 43–68. 1997.

[9] Delhal, J., Ledent, D., Age and evolution of pre-Zadinian migmatitic gneisses, Bas-Zaïre. Annales de la Société Géologique de Belgique, 99, 165–187. 1976.

[10] Delvaux, D., The TENSOR program for paleostress reconstruction. Terra Nova, 5, 216. 1993.

[11] Delvaux, D., Fernandez-Alonso, M., Petroleum potential of the Congo Basin. In: de Wit, M., Guillocheau, F., de Wit, M.C.J. (Eds.), The Geology and Resource Potential of the Congo Basin. Springer, Berlin, pp. 371–391. 2015.

[12] Delvaux, D., Sperner, B., Stress tensor inversion from fault kinematic indicators and focal mechanism data: The TENSOR program. Geological Society, London, Special Publications, 212, 75–100. 2003.

[13] Dott, R.H. Jr., Wacke, graywacke and matrix – What approach to immature sandstone classification? Journal of Sedimentary Petrology, 34(3), 625–632. 1964.

[14] Dunham, R.J., Classification of carbonate rocks according to depositional texture. In: Ham, W.E. (Ed.), Classification of Carbonate Rocks. AAPG Memoir 1, pp. 108–121. 1962.

[15] Eskola, P., The mineral facies of rocks. Norsk Geologisk Tidsskrift, 6, 143–194. 1920.

[16] Foucault, Alain, Jean-François Raoult, Fabrizio Cecca, et Bernard Platevoet. Dictionnaire de géologie. 8e éd. Paris: Dunod, 2014.

[17] Folk, R.L., Practical petrographic classification of limestones. AAPG Bulletin, 43, 1–38. 1959.

[18] Fossen, H., Structural Geology, 2nd ed. Cambridge University Press, Cambridge. 2016.

[19] Gephart, J.W., FMSI: A Fortran program for stress tensor inversion. Computers & Geosciences, 16(7), 953–989. 1990.

[20] Guiraud, M., Laborde, O., Philip, H., Characterization of deformation and stress tensors using microfault analysis. Tectonophysics, 170, 289–316. 1989.

[21] Hancock, P.L., Brittle microtectonics: Principles and practice. Journal of Structural Geology, 7, 437–457. 1985.

[22] Jaeger, J.C., Elasticity, Fracture and Flow with Engineering and Geological Applications. Chapman & Hall, London. 1969.

[23] Means, W.D., A construction for shear stress on a generally oriented plane. Journal of Structural Geology, 11, 625–627. 1989.

[24] Ministère des Hydrocarbures. Atlas des Blocs pétroliers et Gaziers de la République Démocratique du Congo, 1ère Phase des Appels d'Offres. 2022

[25] Müller, B., Reinecker, J., Fuchs, K., The World Stress Map Project. 2000.

[26] Nicholet, J., Reconnaissance géologique et incertitudes en géotechnique. In Actes des Journées Nationales de Géotechnique et de Géologie de l'Ingénieur (JNGG 2010), Grenoble, 7–9 Juillet 2010.

[27] Nicolas, A., Poirier, J.P., Crystalline Plasticity and Solid State Flow in Metamorphic Rocks. Wiley, London. 1976.

[28] Passchier, C.W., Trouw, R.A.J., Microtectonics. Springer, Berlin. 2005.

[29] Lepersonne, J., Carte géologique et notes explicatives de la République du Zaïre, Bruxelles: Musée Royal de l'Afrique centrale, 63 p., 1974

[30] Price, N.J., Cosgrove, J.W., Analysis of Geological Structures. Cambridge University Press, Cambridge. 1990.

[31] Ragan, D. M., Structural Geology: An Introduction to Geometrical Techniques. New York: John Wiley & Sons. 1985.

[32] Ramsay, J.G., Folding and Fracturing of Rocks. McGraw-Hill, New York. 1967.

[33] Ramsay, J.G., Huber, M.I., The Techniques of Modern Structural Geology, Volume 1: Strain Analysis. Academic Press, London. 1983.

[34] Roberts, E.M., Jelsma, R.E., Hegna, T.A., Mesozoic sedimentary cover sequences of the Congo Basin. In: de Wit, M., Guillocheau, F., de Wit, M.C.J. (Eds.), The Geology and Resource Potential of the Congo Basin. Springer, Berlin, pp. 163–191. 2015

[35] Sibson, R.H., Fault rocks and fault mechanisms. Journal of the Geological Society, 133, 191–213. 1977.

[36] Torsvik, T.H., Cocks, L.R.M., The Paleozoic paleogeography of central Gondwana. Geological Society, London, Special Publications, 357, 137–166. 2011.

[37] Twiss, R.J., Moores, E.M., Structural Geology. W.H. Freeman, New York. 1992.

[38] Van Ganse, H.R., Découverte des gisements miniers au Bas-Congo. In: Monographie des ressources minières de la province du Kongo Central. Bas-Congo, République démocratique du Congo. Source historique citée par la Forminière et par des travaux ultérieurs (1950–1980). 1913.

[39] Vernon, R.H., A Practical Guide to Rock Microstructure. Cambridge University Press, Cambridge. 2004.

[40] Winkler, H.G.F., Petrogenesis of Metamorphic Rocks. Springer-Verlag, Berlin. 1974.

Received: February 2026; Revised: February 2026; Accepted: March 2026; Published: March 2026